Numerical modeling to predict threshold fluence for material ejection in laser induced transfer of metals

Divyanshu Bhartiya, M Aanjinappa, Deepak Marla[*]

Indian Institute of Technology, Bombay
Corresponding author: dmarla@iitb.ac.in

Abstract

Laser-induced forwards transfer (LIFT) is one of the most versatile micro-fabrication techniques that finds essential applications in the voxel and 3D printing where it is desirable to work in the solid-state or liquid ejection regimes. Accurate deposition of material demands operating in the proximity of threshold fluence to avoid splashing. Experimental characterization of efficient laser parameters for different metals with varying film sizes proves to be a cumbersome and challenging task. Hence, in the present study, a numerical model encompassing droplet and vapor-induced ejection is developed to emulate the process, explore the concomitant temperature profiles, and put forth an estimate of threshold fluence for a broad spectrum of film sizes. The investigation outcome signifies an enhancement of the metal film temperature with an increase in laser fluence and a decrement with the rise in film thickness and pulse duration due to extensive heat diffusion. Further, it was realized that mere melting is sufficient to bring about material ejection in thinner films, while thicker films require vapor-induced ejection to effectuate deposition. Finally, the threshold fluence for numerous film thicknesses was established, and the results were found well within 10% of the realm of experimental data for thin films (< 600nm).

Keywords: LIFT, thermal-based ejection, vapor-induced ejection, threshold fluence

1. Introduction

Micro-scale fabrication requires high-resolution printing at a minuscule level but finds itself pegged by the challenge of high-temperature implications. Laser-induced forward transfer (LIFT) resolves the prevalent fabrication intricacies with a contactless technique to print materials right away through a bulk solid phase. It entails the competence to deposit an expansive range of materials, single-step printing of multi-layers, development of micro-tracks, and printing of pure substance to find major applications in the digital printing and microelectronics industry. The process was first exhibited in 1986 by Bohandy et al. [1], where an excimer laser pulse (λ: 193 nm) was employed to deposit copper metal (thickness: 0.41 μm) over a fused silica plate stationed in the proximity of the source substrate.

Since its genesis, the technique has been applied for the transfer of numerous materials such as conducting polymer like PEDOT [2], Oxides (Al_2O_3), thin semiconductor (Ge/Si) films, and biomolecules [3]. Yamada et al. [4] investigated the impact of the separation length between the donor and receiver substrate on the quality of material deposition. While several studies have been conducted for LIFT of aluminium films to characterize the ejection mechanism for a range of fluence values and analyze the print quality and its parametric dependence. However, the availability of optimal fluence values for efficient material deposition is still elusive. Although, a conscious effort towards numerical modeling to elucidate the LIFT process, study its underlying principle and define the ejection mechanism has been executed [5]. In one such study, Fardel et al. [6] used the energy balance equation to examine the functioning and responses of the triazene polymer. It was realized that the generation of shock waves plays a significant role in the transfer process but thermal and mechanical processes still largely define LIFT. Despite numerous attempts at numerical modeling, a comprehensive study for the attainment of efficient material ejection remains absent.

Over the years, LIFT has gained recognition for its high-end efficiency, but its proliferation to numerous industries remains unfulfilled due to a lack of effective control over the material transfer. Hence, the current study is an effort to model the heat transfer during the LIFT of a thin metal film and analyze the concomitant temperature variation to establish the threshold fluence for numerous film thicknesses. The attainment of this model is executed by devising a two-dimensional axisymmetric framework encompassing two distinct mechanisms, namely, thermal-based ejection and vapor-induced ejection, to study temperature distribution across different film thicknesses for varying laser intensity. The acquired results are qualitatively examined to dispense significant insights about the laser-material interaction and the consequent ejection. Further, model validation is effectuated through a comparative analysis with experimental data.

2. Model Description

2.1. Thermal Model

The LIFT of metals is predominantly influenced by thermal processes where a laser beam incidents on the top of the glass substrate with intensity I_0, a part of it (R_1) gets reflected to the atmosphere due to the surface properties and electronic structure of the material. The fraction of laser intensity transmitted through the glass layer is reflected (R_2) once again at the interface by the top surface of the metal film (as shown in Fig. 1). The intensity of the laser beam penetrating the top surface of the metal film is:

$$I = (1 - R_1)(1 - R_2)I_0 \tag{1}$$

where R_1 and R_2 denote the reflectivity of glass and metal films respectively.
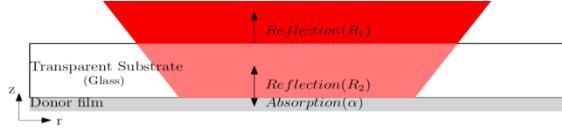

Fig. 1. Schematic of Laser induced forward transfer

The optically penetrated laser beam weakens down along the depth of the metal film, and the absorption across the film determined by the beer-lambert law is formulated as:

$$I(z) = (1 - R_1)(1 - R_2) I_0 \ e^{-\alpha z} \tag{2}$$

where z is the depth of the material from the interface and α is the absorption coefficient of metal.

The absorbed laser energy predominantly impacts the region lying in the proximity of the beam center, where the Gaussian distribution ascertains the variation across the film width. Besides spatial variation, the beam intensity possesses temporal dependence in accordance with a full width half maximum pulse (FWHM). Since the laser beam is cylindrical, the problem can be solved using an axisymmetric geometry, and the governing equations can be defined using cylindrical coordinates. Hence, the ultimate laser beam intensity distribution throughout the volume of the metal film can be written as:

$$I(r, z, t) =$$
$$(1 - R_1)(1 - R_2) I_0 \ e^{-\alpha z} e^{-4ln2\left(\frac{t}{t_p} - 1.5\right)^2} e^{-\left(\frac{r}{2r_0}\right)^2} \tag{3}$$

where r_0 is $(1/e^2)$ beam radius and t_p defines the pulse width at full width half maximum. The pulsed laser beam generates thermal gradients all over the metal film to effectuate heterogeneous temperature distribution and material heating governed by the Fourier's law of heat conduction as depicted below:

$$\rho C \frac{\partial T}{\partial t} = \frac{\partial}{\partial r}\left(k \frac{\partial T}{\partial r}\right) + \frac{\partial}{\partial z}\left(k \frac{\partial T}{\partial z}\right) + S(r,z,t) \tag{4}$$

where $S(r, z, t)$ is the volumetric heat source term defined as the product of the absorption coefficient and the absorbed intensity (given by Eq. 3), illustrated as:

$$S(r, z, t) = \alpha I(r, z, t) =$$
$$\alpha(1 - R_1)(1 - R_2) I_0 \ e^{-\alpha z} e^{-4ln2\left(\frac{t}{t_p} - 1.5\right)^2} e^{-\left(\frac{r}{2r_0}\right)^2} \tag{5}$$

Conversely, the glass substrate transparent to light does not absorb the incident radiation and heats up through the heat transfer between the donor metal and the glass. Hence, the governing equation for heating of the glass film is given by:

$$\rho_g C_g \frac{\partial T_g}{\partial t} = \frac{\partial}{\partial z}\left(k_g \frac{\partial T_g}{\partial z}\right) \tag{6}$$

Where ρ_g, C_g, T_g, and k_g are the density, specific heat, temperature, and thermal conductivity of glass. The boundary conditions for the system are defined on account of the heat flux between glass and metal film as:

$$-k_g \frac{\partial T_g}{\partial z}\Big|_{z=0} = -k \frac{\partial T}{\partial z'}\Big|_{z'=0} \tag{7 (a)}$$

$$T|_{z=L} = T|_{z'=L'} = T_0 \tag{7 (b)}$$

Where L is the domain size of the glass substrate and $L`$ is the domain size of the metal film chosen such that Eq. 7(b) remains satisfied. Eventually, these equations are solved using finite element modeling to furnish the temperature profile for the associated models described in the following section.

2.2. Material Ejection

According to the literature, several mechanisms exist for material ejection depending upon the working laser fluence. In the present study, two of those mechanisms pertaining to liquid ejection are demonstrated through the fabricated model. The first model (Model-1) is established on the ejection caused due to melting of the metal film (as shown in Fig. 2). The molten zone undergoes volumetric expansion due to the density difference originating between the two phases. However, the expansion is restrained by the surrounding until the melt front reaches the bottom free surface, possessing no constraint, where it initiates a protrusion eventuating into a droplet ejection.
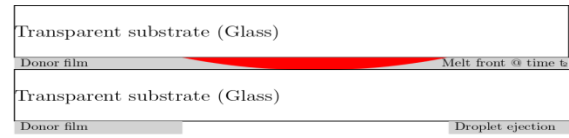

Fig. 2. Droplet ejection mechanism (Model-1)

The second model (Model-2), an extension of the mechanism illustrated in model-1, is formed on vapor-induced ejection where a vapor pocket develops at the metal film and glass substrate interface while the melt front propagates to the free surface (as illustrated in Fig. 3).
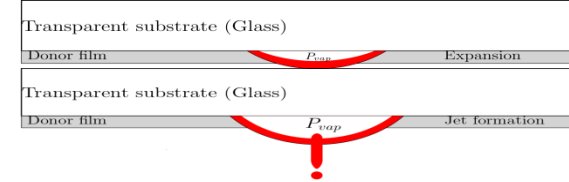

Fig. 3. Vapor-induced ejection mechanism (Model-2)

The pressure force due to the vapor pocket enacts over the molten front to overcome the high viscosity of the melt pool, surface tension, and external pressure. Assuming the droplet to be hemispherical, the value of vapor pressure can be acquired through Young's equation as:

$$P_{vap} = P_{ext} + \frac{2\sigma}{R} \tag{6}$$

Where P_{ext} is the external pressure acting on the film, σ is the surface tension, and R is the radius of curvature for the molten front enumerated equal to the laser beam radius owing to thin-film assumption.

Once the pressure force is adequate, the molten front is ejected and propelled towards the receiver substrate. The required pressure conditions are attained when the laser heating leads the temperature surge to a certain value, which can be extracted through the Clausius-Clapeyron equation as:

$$\ln\left(\frac{P_{vap}}{P_1}\right) = \left(\frac{\Delta H_{vap}}{R_g}\right)\left(\frac{1}{T_{vap}} - \frac{1}{T_1}\right) \tag{7}$$

Where ΔH_{vap} depicts the latent heat of vaporization for the metal, R_g is the universal gas constant, P_1 and T_1 are the reference pressure and temperature conditions, and P_{vap} is the pressure in

the vapor pocket developed due to thermal heating up to a temperature T_{vap}.

2.3. Numerical modeling

The implementation of the ejection models (Model-1 and Model-2) is brought about via developing a two-dimensional axisymmetric model comprising a transient heat transfer study governed by Eq. 4, 5, and 6 to execute the simulational investigation. Two rectangular slabs of width 140 µm and height 1 µm (for glass substrate) and 188 nm - 1073 nm (for the metal film) were constructed and assembled to form the geometry of the system. The slabs were joined via union to define conduction between the two materials, whereas the remaining boundaries were insulated from the external environment, and room temperature (300 K) was designated as the initial condition for the system. A Mesh convergence test was carried out to define a mapped mesh of size 10 nm x 1 µm for the metal film and 20 nm x 1 µm for the glass substrate. A Q-switched YAG laser beam of 532 nm frequency doubled output and radius 30 µm was modeled as a volumetric heat source (defined by Eq. 5) to incident over the center of the material interface. The laser pulse was designated Gaussian distribution in time (FWHM, t_p=15 ns) and space as detailed in Eq. 3. Next, the optical and physical properties of the materials at a wavelength of 532 nm were assigned to the rectangular slabs. Further, it is assumed that the reflectivity falls off rapidly as the temperature of the film approaches the melting temperature; hence, the value of reflectivity is set to be zero post melting point. After performing the simulations, experimental data established by Baseman et al. [8] is utilized for model validation and determining the minimum fluence required for blowing off thin gold films of nanometric scale.

3. Results and discussion

The developed model effectuates laser heating and explores the melting of a metal film and subsequent ejection through the temperature distribution across the layer arising due to the enormous thermal gradients. The generated temperature profile (as illustrated in Fig. 4) for numerous layer thicknesses is studied to analyze the associated heat diffusion mechanism. Ultimately, these thermal contours are deployed to enumerate the threshold fluence for both the models (as discussed in section 2.3) and investigate the temperature variation as a function of fluence and film thickness.
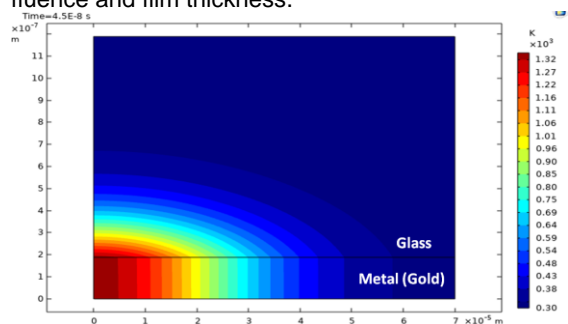

Fig. 4. Contour plot for temperature distribution in a 188 nm film at 45 ns (t_p = 15 ns)

3.1. Temperature variation with pulse width and laser fluence

During LIFT, a large temperature upsurge emanates in the donor layer due to laser heating within short periods. It is observed that for a constant fluence, the film temperature increases with a decrease in pulse width because of rapid heating resulting in larger thermal gradients compared to longer pulses with large diffusion lengths (see Fig. 5). Further, it was noticed that upon holding the pulse width constant, an increase in laser fluence boosts up the temperature growth rate, and the temperature rise is perceived to be linear. At lower fluences, the entire layer of metal film undergoes melting, indicative of droplet ejection at the receiver substrate. While, at higher fluence, the material undergoes superheating and vaporization, suggestive of splashing instead of droplet formation. Thereby, it is inferred that the donor layer endures a molten regime at lower fluences and progresses to a vapor regime at higher fluences.
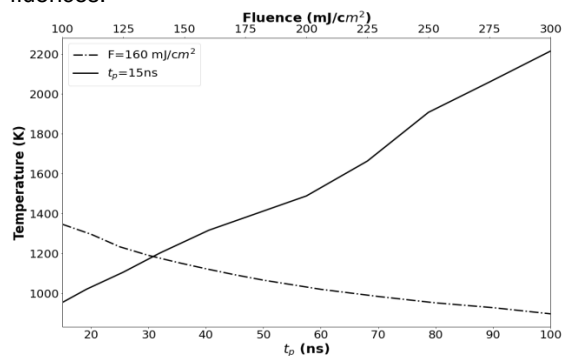

Fig. 5. Temperature variation with pulse width and fluence for 188 µm thick gold film

3.2 Temperature variation with film thickness

However, it is noted that the disparity across the donor layer is also attributed to the film thickness. Deductions from the simulation results show that for constant laser fluence, the peak temperature decreases with an increase in film thickness, signifying that a larger amount of energy is required to melt a thicker donor film (see Fig. 6). Further, the temperature across a thinner donor layer depicts minute variations due to a high thermal diffusion length for the employed nanosecond pulse (see Fig .6: variation along depth). While a thicker layer shows a noticeable temperature difference due to the extensive heat diffusion along the depth among thicker films leading to lower thermal gradients than the thinner ones. Moreover, it is also observed that a greater molten pool develops for larger films suggesting an enhanced droplet deposition. Whereas insignificant heat dispersion is detected in the glass substrate because of its low thermal diffusivity. Overall, the variance in temperature distribution illustrates that there prevails a limit of film thickness for a certain laser fluence that could be irradiated to effectuate droplet ejection. Such a combination of the fluence value with its limiting film thickness establishes the threshold fluence for the donor layer.
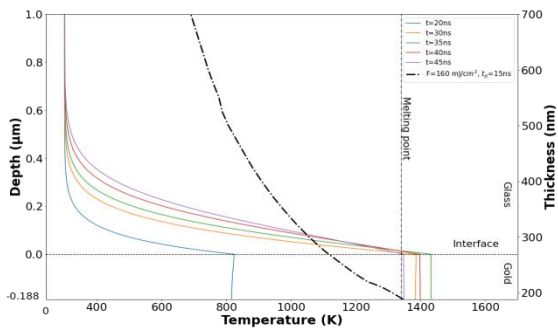
Fig. 6. Temperature variation along depth of a 188 μm thick gold film at different time intervals (at threshold) and with various films irradiated with a fluence = 160 mJ/cm² at t_p = 15 ns (dash-dotted line)

3.3. Comparison with experiments

The threshold fluence values fetched from the simulations for different donor layers are delineated in Figure. 7 along with experimentally acquired values from the literature [7]. The plot is employed to corroborate the model results against the experimental data and lay out a proposition regarding the ejection mechanism for different ranges of fluence and film thickness conditions. It can be observed that the threshold estimates from model-1 lie in close proximity to the experimental values for thinner films, indicating that the ejection mechanism at lower thickness is primarily melting based where the entire film undergoes melting and leads to droplet ejection.
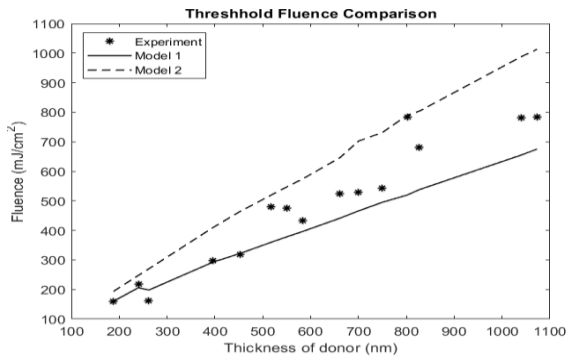

Fig. 7. Comparison of threshold fluence obtained from the models with experimental data

However, as the film thickness grows, a divergence is detected between the experimental and simulated data (model-1), suggesting that several other factors govern the material ejection for larger donor layers. At thicker films, threshold values predicted by model-2 tend to approximate the experimental values to some degree (within 18% of the experimental data). Correspondingly, it can be deduced that larger films call for vapor pressure developed at the interface to overcome the external pressure, surface tension, and viscous forces to effectuate material ejection, while mere melting of the film is insufficient to cause the deposition. Therefore, the developed models work in tandem to produce a good estimate regarding the ejection regimes for different donor layers and subsequently dispense an adequate approximation about the threshold fluence values.

4. Conclusions

LIFT of metals comprises several complex physical phenomena which cause difficulty in modeling the process accurately due to the involved intricacies. However, with the approach proffered in the present study, it is possible to comprehend the involved heat transfer phenomenon, temperature distribution across the donor film, and concerned ejection mechanisms. The simulational studies illustrate that for film thickness below 600 nm, the threshold fluence increases linearly and the values registered are less than 500 mJ/cm². It is further observed that this increase in laser fluence results in a linear surge in the peak temperature of the donor layer as well. While for a thicker film, the threshold fluence soars rapidly owing to the need for more energy to effectuate material ejection. Due to extensive heat diffusion across the layer, thicker films possess a large melt pool, leading to substantial temperature disparity along the depth of the thicker film in contrast to a thinner film. On the other hand, the ejection mechanism can be predicted by analyzing the combination of fluence, film thickness, and the pulse duration employed for deposition. The results acquired from the developed model are well within the 10% range of the experimental data for thinner films. However, it falls short on accuracy for predicting threshold values for larger films due to possible solid-state ejection transpiring during the process and not accounted for in the model. Altogether, the established models dispense preliminary results and subsequently provide an idea about the threshold fluence window for different layer thicknesses and define the associated ejection regimes.

References

[1] Bohandy, J., et al. "Metal deposition from a supported metal film using an excimer laser." Journal of Applied Physics 60.4 (1986): 1538-1539.
[2] Piqué, Alberto. "Laser transfer techniques for digital microfabrication." Laser Precision Microfabrication (2010): 259-291.
[3] Hopp, Béla, et al. "Femtosecond laser printing of living cells using absorbing film-assisted laser-induced forward transfer." Optical Engineering 51.1 (2012): 014302.
[4] Yamada, H., et al. "Optimization of laser-induced forward transfer process of metal thin films." Applied surface science 197 (2002): 411-415.
[5] Kantor, Z., et al. "Laser induced forward transfer: The effect of support-film interface and film-to-substrate distance on transfer." Applied Physics A 54.2 (1992): 170-175.
[6] Fardel, Romain, et al. "Energy balance in a laser-induced forward transfer process studied by shadowgraphy." The Journal of Physical Chemistry C 113.27 (2009): 11628-11633.
[7] Baseman, Robert J., et al. "Minimum fluence for laser blow-off of thin gold films at 248 and 532 nm." Applied physics letters 56.15 (1990): 1412-1414.